Journal of Chromatography A, 1217 (2010) 1208–1218

Contents lists available at ScienceDirect

Journal of Chromatography A

journal homepage: www.elsevier.com/locate/chroma

Solid phase extraction of copper(II) by fixed bed procedure on cation exchange complexing resins

Maria Pesavento*, Michela Sturini, Girolamo D'Agostino, Raffaela Biesuz

Dipartimento di Chimica Generale, Università di Pavia, Via Taramelli 12, 27100 Pavia, Italy

ARTICLE INFO

Article history:
Received 16 October 2009
Received in revised form 4 December 2009
Accepted 9 December 2009
Available online 16 December 2009

Keywords:
Solid phase extraction
Metal ions
Copper(II)
Complexing resins
Adsorption equilibria on complexing resins
Adsorption kinetics on complexing resins

ABSTRACT

The efficiency of the metal ion recovery by solid phase extraction (SPE) in complexing resins columns is predicted by a simple model based on two parameters reflecting the sorption equilibria and kinetics of the metal ion on the considered resin. The parameter related to the adsorption equilibria was evaluated by the Gibbs–Donnan model, and that related to the kinetics by assuming that the ion exchange is the adsorption rate determining step. The predicted parameters make it possible to evaluate the breakthrough volume of the considered metal ion, Cu(II), from different kinds of complexing resins, and at different conditions, such as acidity and ionic composition.

1. Introduction

Complexing resins are widely used for metal ions separation since the pioneering work of Riley and Taylor [1], because of their high specificity and sorbing strength for those metal ions which are complexed by the active groups present in the resin. Dynamic solid phase extraction (SPE) based on complexing resins is widely diffused for separation and preconcentration of metal ions from complex matrices, allowing the recovery of even strongly linked metal ions [2]. It has been used for reducing matrix interferences for example before spectroscopic determination of metals in seawater [3], or before ICP-MS determination [4]. Separations and preconcentrations before HPLC or CE have been reported too, to improve the detection limits [5,6]. In this context it is interesting to predict the loading behaviour of metal ions on SPE columns or cartridges and in particular the maximum sample volume which can be fed to the column without losing solute. Some typical breakthrough (bt) curves, obtained for copper(II) on short columns containing complexing resins, are shown in Fig. 1.

The breakthrough volume (V_b) is the eluted volume for which a low fraction of metal ion emerges from the column. It depends on the position of the curve along the volume axis and on the dispersion of the elution front. Various numerical models have been proposed for the breakthrough curves, based on adsorption isotherms as the Langmuir isotherm, giving a good reproduction of the elution profiles [7–9]. Thermodynamic parameters fix the retention volume (V_R), corresponding to the inflection point of the bt curve, while the mass transfer kinetics determines its shape.

In the present research a similar but much simpler model is applied for describing the elution profile [10–12]. Two macroscopic parameters characterize the bt curves, related respectively to the adsorption equilibrium and kinetics, as in the model mentioned above. The first one is the retention volume (V_R), i.e. the volume required to half of the original metal concentration to emerge from the column [13–15]. It is related to the distribution coefficient D by the following relationship [16]:

$$V_R = V_m + DV_s \quad (1)$$

which has been successfully used in several chromatographic techniques, as for example for the reversed phase partition chromatography [17]. D is the distribution coefficient, i.e. the ratio of the concentration of the metal ion in the solid phase (in mmol mL_s^{-1}) and in the solution phase (in mmol mL^{-1}), in all its chemical forms, at equilibrium. V_m and V_s are the mobile and solid phase volume in the column.

The distribution coefficient is an equilibrium parameter, describing the distribution equilibrium between two phases, which is most often obtained by the Langmuir isotherms. However the parameters of the Langmuir equation depend on the conditions, so they are not really predictive. Better prediction of the distribution coefficient D in a wide range of conditions can be obtained based on the Gibbs–Donnan model of the ion exchange resin [18–20].

* Corresponding author. Tel.: +39 0382987580; fax: +39 0382528544.
E-mail address: maria.pesavento@unipv.it (M. Pesavento).

0021-9673/$ – see front matter © 2009 Published by Elsevier B.V.
doi:10.1016/j.chroma.2009.12.030

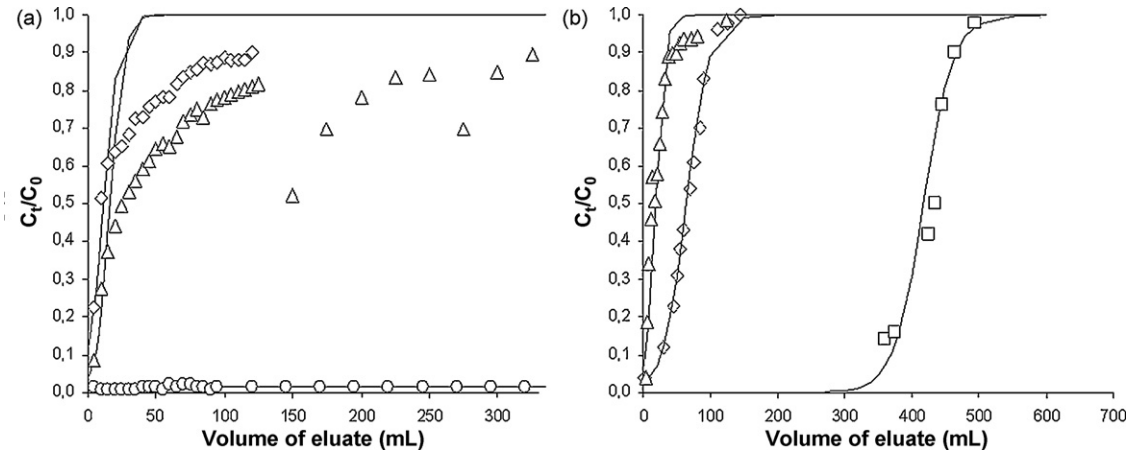

Fig. 1. Breakthrough profiles of copper(II) on complexing resin. (a) IC Chelate (0.073 g of dry resin) at different pH; 0.1 M $NaNO_3$, $C_{Cu} = 2.4 \times 10^{-5}$ M, $C_{IDA} = 5.0 \times 10^{-2}$ M, flow rate 0.8 mL/min; ◊: pH 1.95; △: pH 2.68 (flow interruptions at 125 mL for 5 h and 250 mL for 3 h); ○: pH 8.36. (b) Amberlite CG 50 in the presence of ligands; 0.1 M $NaNO_3$; △: 0.500 g of dry resin, $C_{Cu} = 5.0 \times 10^{-6}$ M, ethylenediamine 1.0×10^{-3} M, pH 3.97, flow rate 1 mL/min; ◊: 0.200 g of dry resin, $C_{Cu} = 5.0 \times 10^{-6}$ M, glycine 5.0×10^{-4} M, pH 6.70, flow rate 1 mL/min; □: 0.198 g of dry resin, $C_{Cu} = 5.0 \times 10^{-6}$ M, IDA 1.0×10^{-4} M, pH 4.4, flow rate = 0.95 mL/min (flow interruption at 13.9 mL for 18 h) Continuos lines calculated as described in the text.

According to this model the resin phase can be considered as a pseudo-solution in which the active groups are immobilized, but interact with protons and metal ions. The counter ions not linked to a specific site are free in the resin phase. The Gibbs–Donnan model will be here applied for prediction of the retention volume, according to Eq. (1).

The volume for which the metal ion emerges from the column, i.e. the bt volume (V_b), depends not only on the half exhaustion point (V_R), but also on the dispersion of the analyte inside the column at the front of eluate, determined by the kinetics of the mass transfer process if axial and edge diffusion are less important. In the present work this point is checked by comparing the sorption kinetics in column with that determined by batch procedure. In both cases ion exchange is assumed to be the rate determining step [21].

A large number of organic and organofunctionalized ion exchange and complexing materials have been proposed so far as stationary phase, and several columns containing complexing resins are commercially available. In the present work two iminodiacetic resins, IC Chelate and Chelex 100 and a carboxylic resin, Amberlite CG 50 were considered. The first two resins have a similar morphology, both being microporous, while Amberlite CG 50 is a macroporous resin, as seen in Fig. 2. The equilibrium characteristics of the copper(II) adsorption on these resins, described by the Gibbs–Donnan model, are well known [22,23]. For this reason copper(II) was here examined as case metal ion.

1.1. Modelling the breakthrough curves

The simplified Thomas and Adams-Bohart models have been successfully used to describe the sorption in different systems, as anions (chromate) on anionic exchange resins [24], neutral molecules (phenol) on activated sludge [25], precious metal ions on cross-linked chitosan [10], proteins on composite silica-polyacrylamide gel ion exchanger (HyperD) [26], and metal ions on strong cation exchanging resins [11]. In this case it has been assumed that the rate limiting step of the sorption process is the ion exchange [11,12]:

$$2\bar{B} + M^{2+} \rightleftarrows \bar{M} + 2B^{+} \quad (2)$$

Eq. (2) is a modification of the previously proposed sorption reaction [11,12]. In the case of complexing resins, in which the charged group is a weak acid, as $–NH^+$, or a weak base as $–COO^-$, the counter ion in the resin can be free or it can be linked to the active group, as for example in the case of protons to weak basic groups, or metal ions to metal complexing groups. The relationship relating the eluted volume V with the concentration is [11,12]:

$$\frac{C}{C_0} = \frac{1}{1 + \exp[(kC_0/Q)((q_e w/C_0) - V)]} \quad (3)$$

where C is the outlet metal ion concentration at eluted volume V, C_0 is the inlet concentration (mol L^{-1}), w is the amount of resin in the column (g), Q is the volumetric flow rate (mL min^{-1}) and q_e

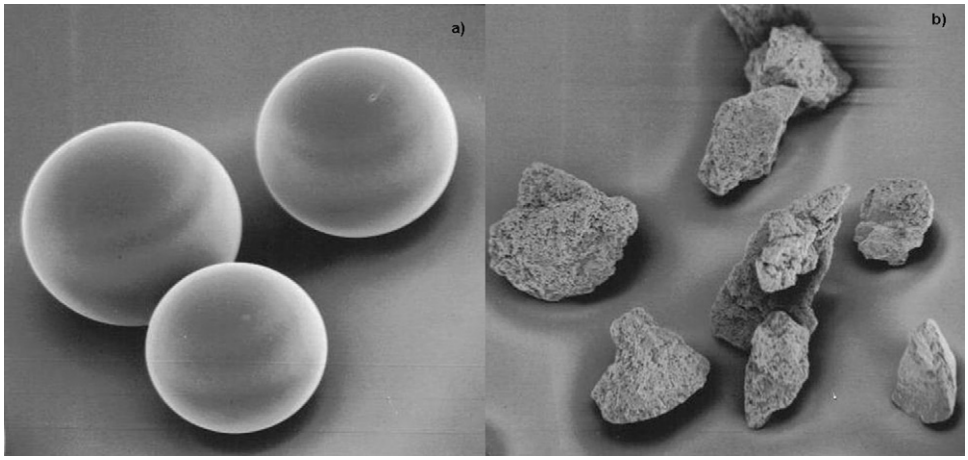

Fig. 2. Pictures of IC Chelate in (a) and Amberlite CG50 in (b), obtained with a scanning electronic microscope, Cambridge stereoscan, Au 100 Å sputtering.

($\mathrm{mmol\,g_s^{-1}}$) is the metal ion concentration in the resin in equilibrium with a concentration C_0 in solution. The parameter $q_e w/C_0$ (mL) is the volume for which $C/C_0 = 0.5$, i.e. the retention volume V_R. It is related to the distribution coefficient D by the following relationship:

$$V_R = \frac{q_e w}{C_0} = DV_s \tag{4}$$

which is equal to Eq. (1) if V_m is negligible with respect to DV_s, as it is usually the case. D and V_R can be predicted from the sorption equilibria as described below.

The second parameter of Eq. (3), kC_0/Q, depends on the adsorption kinetics [11,12]. As a matter of fact kC_0 has the dimension of a first order rate constant ($\mathrm{min^{-1}}$).

Complete models have been proposed for describing the ion exchange kinetics [16], but the most useful ones for practical applications are those based on some simplifying assumptions about the rate determining step. Considering the ion exchange reaction (Eq. (2)) as rate determining in the case of the adsorption of metal ions on complexing resins, the rate of the mass transfer process by static contact procedure is [21,27]:

$$\frac{dq_t}{dt} = k_f[\bar{B}]^2\left(C_0 - q_t\frac{w}{V}\right) - k_b C_B^2 q_t \frac{w}{V_s} \tag{5}$$

q_t is the concentration of metal ion in the resin phase ($\mathrm{mmol\,g_s^{-1}}$) at time t, V is the volume of the solution phase and V_s is the volume of the solid phase. k_f and k_b are the forward and reverse kinetic constants of reaction (2). $[\bar{B}]$ indicates the concentration of a monovalent counter ion not linked to the active groups in the resin phase, in $\mathrm{mmol\,g_s^{-1}}$, and C_B is the concentration of a monovalent counter ion in the solution phase, in $\mathrm{mmol\,mL^{-1}}$. In the present investigation the monovalent counter ion was Na^+, at constant concentration in the solution phase, usually 0.1 M and sometimes 1 M. The counter ion concentration in the resin is constant at constant acidity, as far as the amount of complexable metal ions is negligible with respect to the total active groups in the resin phase. Considering that at equilibrium $dq_e/dt = 0$, q_e being the concentration of the metal ion in the resin phase (in $\mathrm{mmol\,g_s^{-1}}$) at equilibrium, C_0 can be evaluated. Substituting in Eq. (5), the following relationship is obtained

$$\frac{dq_t}{dt} = \left(k_f[\bar{B}]^2\frac{w}{V} + k_b C_B^2\frac{w}{V_s}\right)(q_e - q_t) \tag{6}$$

The kinetic constant is

$$k_k = k_f[\bar{B}]^2\frac{w}{V} + k_b C_B^2\frac{w}{V_s} \tag{7}$$

k_k has the dimensions of a first order equation kinetic constant, $\mathrm{min^{-1}}$, as kC_0 in Eq. (3). It can be predicted from k_f and k_b if C_B and $[\bar{B}]$ are known. The integration gives this relationship, from which the kinetic constant can be evaluated:

$$\ln(1 - X) = -k_k t \tag{8}$$

where $X = q_t/q_e$ is the fractional approach to equilibrium [28]. The forward and backward kinetic constants can be evaluated by investigation at different counter ion concentration.

1.2. Prediction of the adsorption equilibria of metal ion on complexing resins

The Langmuir and/or Freundlich isotherms which are most often used to describe the sorption equilibria on ion exchange and complexing resins, are not predictive, since the parameters, for example the pH and the ionic strength change with the conditions [27]. Moreover the Langmuir isotherm is valid for monolayer sorption onto a surface by combination with a finite number of identical sites. This is not always true in the case of complexing resins, in which a number of complexing groups, differently protonated, can coordinate the metal ion. A method for the evaluation of the distribution coefficient in a wide range of different conditions, and in the presence of different complexation sites has been proposed, based on the Gibbs–Donnan model of the resin [18,22]. The resin is considered as an aqueous phase containing fixed groups able to complex metal ions. Since these groups are often protonated, the complexation reaction in the resin phase can be written as:

$$\bar{M} + \overline{H_xL} \rightleftarrows \overline{MH_zL} + q\bar{H} \tag{9}$$

$$K_i = \frac{[\overline{MH_zL}][\bar{H}]^q}{[\bar{M}][\overline{H_xL}]}$$

The species with the overbar are those in the resin phase. K_i is the complexation constant in the resin phase, and according to the Gibbs–Donnan model should be equal to the corresponding equilibrium constant in solution. The concentration of the x-protonated groups H_xL in the resin is calculated from the side reaction coefficient of the species H_xL, $\overline{\alpha_{H_xL}}$, which is evaluated from the known protonation equilibria of the active groups, as extensively reported elsewhere [22]:

$$\overline{\alpha_{H_xL}} = \frac{\sum_0^r[\overline{H_iL}]}{[\overline{H_xL}]}$$

r is the maximum number of protons that can be linked to each active group. Assuming that the main driving force for the adsorption of a metal ion is its complexation by the active groups in the resin, the corresponding adsorption equilibrium is

$$M + \overline{H_xL} \rightleftarrows \overline{MH_zL} + qH; \quad K_{ex} = \frac{[\overline{MH_zL}][H]^q}{[M][\overline{H_xL}]} \tag{10}$$

K_{ex} can be evaluated from K_i by applying the Donnan equilibrium at the resin–solution interface [22,23] to evaluate the metal ion concentration in the resin phase:

$$K_{ex} = K_i\frac{[B]^{q-m}}{[\bar{B}]^{q-m}} \tag{11}$$

B is a monovalent counter ion, a cation in the case of the complexing resins here considered, not complexed by the groups inside the resin and m is the charge of the metal ion complexed by the active groups in the resin. If complexable metal ions are present at trace level, the concentration of the counter ion in the resin phase can be calculated from the deprotonation degree (β) of the active groups in the resin, i.e. the ratio of the concentration of the deprotonated (L) to total active groups in the resin:

$$\beta = \frac{[\bar{L}]}{\sum_0^r[\overline{H_xL}]} = \frac{1}{\sum_0^r\overline{K_{ay}}[H]^y} \tag{12}$$

$\overline{K_{ay}}$ are the apparent protonation constants of the complexing groups in the resin. The partition coefficient of the metal ion, λ' ($\mathrm{mL\,g_{res}^{-1}}$), is the ratio of the concentration of all the metal species in the resin phase ($q_e = \sum_1^u[(\overline{MH_zL})_l]$, summation extended to all the u species in the resin) to the free metal ion in solution ([M]), at equilibrium conditions:

$$\lambda' = \frac{q_e}{[M]} = \frac{\sum_1^u[(\overline{MH_zL})_l]}{[M]} = \sum\frac{K_{ex,l}\overline{c_L}}{[H]^q\overline{\alpha_{H_xL}}} \tag{13}$$

$\overline{c_L}$ is the total concentration of free complexing groups in the resin phase. The summation is extended to all the metal species formed in the resin phase. The ratio of the activity coefficients in the resin is assumed to be equal to 1, while the activity coefficients in solution are evaluated by the Debye–Huckel extended equation. The partition coefficient can be evaluated at many different conditions,

as for example pH and ionic strength, by Eq. (13). The distribution coefficient D depends on the partition coefficient and on the side reaction coefficient of the metal ion in solution:

$$D = \frac{\lambda' w}{\alpha_M V_s} \quad (14)$$

α_M, i.e. the side reaction coefficient of the metal ion in solution, is the ratio of the total to free metal ion in solution. In the present investigation λ' is calculated by Eq. (13) from the adsorption equilibria of copper(II) on the complexing resins, which were known from previous investigations [22,23,29]. The model described is particularly convenient when some simplifying assumptions can be made. For example, the concentration of free active groups in the resin can be considered equal to the total concentration, since the complexing groups are in large excess with respect to the metal ion in resin phase. Another approximation is that in all the acidity range investigated, 1 g of water is adsorbed per gram of resin, and that the density of the solid phase is always 1 g mL_s^{-1}. Actually this is only a rough approximation since the water adsorbed by unit mass of resin depends on the deprotonation degree [22].

While λ' can be predicted merely from the adsorption equilibria, D requires also the knowledge of the complexation of metal ion in solution. On the other hand α_M can be evaluated from experimental D if λ' is known [14,30].

Eq. (13) shows that the concentration of free metal ion M can be evaluated from the concentration of metal ion adsorbed on the resin at equilibrium [31]. Since in dynamic procedures the equilibrium between the stationary phase and the solution is reached when the effluent concentration is equal to that of the influent [7,8,32–34], the free metal ion concentration in the original solution, i.e. at C_0, can be evaluated from Eq. (13) by fixed bed procedure, if λ' and q_e, the metal ion concentration in the resin phase at equilibrium, are known.

2. Experimental

2.1. Materials and reagents

All chemicals were analytical reagent grade. Milli-Q purified water (Millipore, USA) was used. Solutions were equilibrated for at least one day before use to allow complete equilibration between copper(II) and ligands.

The complexing resins IC Chelate (Alltech Italia srl) and Chelex 100 (Bio-Rad, Richmond, Ca, USA), with a particle size of 100–200 mesh (70–100 μm), were delivered in sodium form. They were washed with HNO_3 1 mol L^{-1}, in batch, stirring for 24 h in order to exchange Na^+ with H^+. Then they were washed with Milli-Q water with successive portions until the pH of the washings was 4.5. Amberlite CG 50 (Sigma–Aldrich), delivered in H^+ form, was treated similarly to the iminodiacetic resins. The maximum capacity, corresponding to the number of active groups (L) per g of dry resin, is 2 and 10 mmol g^{-1} for the iminodiacetic and carboxylic resin respectively [22,23].

2.2. Apparatus

A PerkinElmer 100B flame AAS and a Shimadzu AA-6601G/GFA 6500 spectrophotometer ETAAS were used for copper determination. The operating conditions and the instrumental parameters were those suggested by manufacturers. The linearity range was 0.1–5 mg L^{-1} (LOD 0.2 mg L^{-1}) and 1.57×10^{-8} to 7.87×10^{-8} mol L^{-1} (LOD 0.47×10^{-8} mol L^{-1}) respectively for AAS and GFA, determined according to the recommendation of the manufacturers. The detection limit was twice the concentration of the standard sample that gives an absorbance of approximately 0.0044, multiplied R/S, where R is the highest blank signal and S is the absorbance of the standard (average of ten replicate analyses). All the determinations were done in HNO_3 0.5 mol L^{-1}.

The pH of the solutions was measured with a combined Orion glass electrode 9102 SC, standardized in H^+ activity.

Solutions were delivered to the column with a peristaltic pump (Gilson, Minipuls3) through Teflon tubes previously washed with HNO_3 1 mol L^{-1} and conditioned with a solution of the same composition of the sample. The fractions were collected by a fraction collector 2110 Model, Bio-Rad. The experiments were carried out in an air conditioned room at 20 ± 1 °C, and some times at different temperatures.

2.3. Column procedure

Glass and polypropylene tubes (Bio-Rad), with an internal diameter of 0.5–1 cm, equipped with polyethylene frits and a removable polyethylene stopcock, were used to prepare the columns. The tubes were filled with a slurry of cleaned resins (0.07–0.65 g of dry resin) suspended in MilliQ water. Before connecting the column, the apparatus was fluxed with 50 mL of HNO_3 0.1 mol L^{-1}, and then conditioned with a solution containing only the background electrolyte (0.05–0.1 mol L^{-1} $NaNO_3$) adjusted to the appropriate pH with concentrated nitric acid or solid sodium carbonate, at a flow rate of 2 mL/min. 150–200 mL of mobile phase were required to obtain a pH in effluent solution equal to that of the influent within 0.05 units. The pH of the effluent solution was monitored every 10 mL. The sample was fed to the top of the column at a flow rate 0.2–1 mL min^{-1}. Effluent fractions (5–10 mL) were acidified with HNO_3 0.1 mol L^{-1} before analysis by atomic spectroscopy. The volume of fractions was measured by weighting. At the end of the experiment the column was washed with 1 mL of 0.05 mol L^{-1} ammonium acetate, and the metal ion adsorbed was recovered with 40 mL of HNO_3 0.5 mol L^{-1}. The dynamic capacity of the resin, i.e. the mmol of copper(II) adsorbed per g of dry resins at equilibrium conditions, was determined from the experiments for which a constant concentration of copper(II) in the effluent was obtained.

2.4. Batch procedure

Different portions of resin (0.10–0.50 g of dry resin in H^+ form) were contacted with individual 30 mL volumes of aqueous solution, 0.1 M $NaNO_3$, containing copper(II) and sometimes IDA as ligand, under stirring on a rotating plate at 70–300 rotation per minute, which was sufficient to maintain the suspension. The appropriate pH was obtained with concentrated NaOH and nitric acid, and controlled by pHmeter. The sorption was carried out up to equilibration, i.e. at constant concentration of the metal ion in solution. After selected contact times, small volumes of the liquid phase, 0.1 mL were separated with a filtration syringe, acidified with HNO_3 and the metal ion in solution measured by AAS or GFA.

Experiments were carried out in an air conditioned room, at different temperatures from 17 to 25 °C, with an uncertainty of 1 °C.

3. Results and discussion

Some typical bt profiles of Cu(II) on column of iminodiacetic resin IC Chelate and carboxylic resin (Amberlite CG50) are shown in Fig. 1a. The experimental details of these and other experiments are reported in Table 1. The experiment at pH 8.36 in Fig. 1 was carried out with IC Chelate. In this case the calculated retention volume (Eqs. (4) and (14)) was 3.4×10^{19} mL even if the column was relatively small. A complete elution profile can be obtained in a reasonable time, a few hours at most, only in experiments at much lower pH.

All the sorption profiles of copper(II) from Amberlite CG 50 are symmetrical around V_R, while those from iminodiacetic resins are

Table 1
Experimental conditions for the investigation of the adsorption of copper(II) on small complexing resins columns.

Experiment	T (°K)	Dry resin (g)	V_{col} (mL)	c_{Cu} (M)	c_{Ligand} (M)	pH	Flow rate (mL min^{-1})
IC Chelate							
1[a]	290	0.073	0.1	1.25×10^{-5}	2.50×10^{-2}	2.75	0.2
2	290	0.106	0.2	2.40×10^{-5}	5.00×10^{-2}	3.00	1.0
3	290	0.106	0.2	2.40×10^{-5}	5.00×10^{-2}	3.52	1.5
4[a]	293	0.073	0.1	1.25×10^{-5}	2.50×10^{-2}	1.96	0.2
5[a]	293	0.073	0.1	1.25×10^{-5}	2.50×10^{-2}	1.96	0.2
6	293	0.073	0.1	2.40×10^{-5}	5.00×10^{-2}	2.00	0.2
7	293	0.133	0.2	2.40×10^{-5}	5.00×10^{-2}	2.25	1.0
8	293	0.153	0.3	2.70×10^{-7}	5.00×10^{-2}	2.40	0.8
9[a]	293	0.073	0.1	1.25×10^{-5}	2.50×10^{-2}	2.75	0.8
10	303	0.168	0.3	2.39×10^{-5}		1.30	1.0
11	303	0.073	0.1	2.40×10^{-5}	5.00×10^{-2}	2.00	0.8
12	303	0.073	0.1	2.40×10^{-5}	5.00×10^{-2}	2.68	1.0
13	303	0.156	0.3	2.40×10^{-5}	5.00×10^{-2}	2.40	0.8
Chelex 100							
1	rt	0.651	1.2	2.40×10^{-5}		1.20	0.8
2	rt	0.651	1.2	2.40×10^{-5}	5.00×10^{-2}	2.20	0.8
3	rt	0.250	0.5	9.00×10^{-5}		1.30	1.0
4	rt	0.250	0.5	9.00×10^{-5}		1.50	1.0
Amberlite CG 50							
1	rt	0.500	1.9	5.00×10^{-6}	1.00×10^{-3}	3.97	1.0
2	rt	0.198	0.6	4.90×10^{-6}	1.00×10^{-4}	4.40	1.0
3[b]	rt	0.200	1.2	5.00×10^{-6}	5.00×10^{-4}	6.70	1.0

rt: Room temperature.
[a] 0.05 M $NaNO_3$.
[b] 1.00 M $NaNO_3$.

considerably steeper in the first than in the second part, as seen for example in Fig. 1b. Moreover in the experiments with IC Chelate a large drop in the emerging concentration is observed when the flux is interrupted in column for some hours. The concentration drop increases with increasing interruption time. The same effect was observed with Chelex 100, while not with Amberlite CG 50, where it is not distinguishable from the experimental uncertainty. Breakthrough profiles with a discontinuity after a flow interruption, similar to that observed for IC Chelate, have been reported [35,36] when different diffusion regions are present. In the case of microporous resins IC Chelate and Chelex 100 the mobility of the ions in the micropores is lower than that in the outer particle film, which is the only diffusion region in the case of the macroporous Amberlite CG 50. The morphological difference is clearly seen in Fig. 2. The shape of the whole bt curve is well reproduced by Eq. (3) in the case of Amberlite CG 50, while not in the case of the iminodiacetic resins. Here the two parts of the bt curves were independently treated by Eq. (3), so that two values of the kinetic parameter kC_0 were obtained, one for each part of the bt curve. The part of the bt profile at lower eluted volumes is interesting for predicting the bt volume. The shape of the second part of the elution profile determines the attainment of steady state conditions. The results are summarized in Table 2. The continuous curves in Fig. 1 were calculated by Eq. (3) with V_R evaluated from the Gibbs–Donnan equilibrium model and the kinetic parameter obtained experimentally from Eq. (3) in the first part of the bt profile only in the case of the iminodiacetic resins. The experimental data in the first part of the bt curve are well reproduced by Eq. (3). Other more complex models for unsymmetrical bt curves have been proposed, for example the equilibrium-dispersive model when the efficiency of the column decreases with increasing concentration in the solution phase [7].

3.1. Adsorption equilibria in column

The retention volume depends on the adsorption equilibria according to Eq. (1). It can be obtained directly from the bt curve, at $C/C_0 = 0.5$, or as a parameter of Eq. (3). In the case of the iminodiacetic resins the two V_R values obtained in the two parts of the elution curve, V_{RI} and V_{RII}, were similar as seen from the regression line:

$$V_{RII} = -6(9) + 1.6(2)V_{RI}; \quad r^2 = 0.80 \quad (n = 11)$$

This similarity indicates that the same adsorption equilibria take place in the two parts of the elution curve and that the different shape is due to the kinetics.

The values of V_R obtained by Eq. (3) correspond well to those obtained from the bt profile, at $C/C_0 = 0.5$, which are reported in Table 2. They can be compared with V_R calculated by Eq. (1) (V_{Rcalc}), using D evaluated from the Gibbs–Donnan model of the resin by Eq. (14), which are reported in Table 2. The partition coefficients λ' used for this evaluation are reported in Table 2 too. They were evaluated from the protonation and exchange coefficients of the complexing resins according to Eq. (13). The internal constants (K_i) of IC Chelate are equal to those of Chelex 100, as expected since the same complexing groups at the same concentration are present in the two resins. D depends on the side reaction coefficient of the metal ion in solution, α_{Cu} (Eq. (14)) which measures the extent of the metal complexation in the solution. The side reaction coefficients reported in Table 2 were obtained from the protonation and complexation constants of iminodiacetic acid [22], and the other ligands considered [29] reported in the literature. The speciation code MEDUSA [37] was used for the evaluation of the side reaction coefficients. In the absence of ligand the side reaction coefficient is equal to 1.

The retention volumes calculated from D according to Eq. (1) (V_{Rcalc}) and those obtained experimentally from the bt curves (V_{Rexp}) are not significantly different:

$$V_{Rexp} = -31(12) + 1.4(2)V_{Rcalc}; \quad r^2 = 0.87 \quad (n = 20)$$

In this comparison all the experiments in Table 1 were considered, independently of the temperature. Indeed, the variation of the equilibrium parameters with temperature is low for a relatively small temperature range around the room temperature, as that here considered [38]. The complexation constants used for the evaluation were obtained at 25 °C.

Table 2
Equilibria and kinetics of the adsorption of copper(II) on complexing resins determined from the bt profiles from small complexing resins columns. The experimental conditions are in Table 1.

Experiment	α_{Cu}	λ'	D	V_R(bt)	V_{Rcalc}	kC_0 (I)	kC_0 (II)
IC Chelate							
1	226.9	3.50×10^5	1.15×10^3	110	113	2.03×10^{-2}	2.46×10^{-3}
2	759.8	9.37×10^5	9.17×10^2	95	131	3.53×10^{-2}	1.47×10^{-2}
3	3232.5	5.41×10^6	1.24×10^3	255	177	5.45×10^{-2}	2.68×10^{-2}
4	14	9.65×10^3	5.16×10^2	27	50	5.37×10^{-2}	1.11×10^{-2}
5	14	9.65×10^3	5.16×10^2	30	50	4.65×10^{-2}	6.15×10^{-3}
6	23.7	1.03×10^4	3.25×10^2	17	32	2.92×10^{-2}	5.69×10^{-3}
7	62	3.20×10^4	3.98×10^2	56	69	7.13×10^{-2}	2.35×10^{-2}
8	107.7	6.35×10^4	4.45×10^2	170	90	5.33×10^{-2}	6.81×10^{-3}
9	226.9	3.50×10^5	1.15×10^3	75	113	9.97×10^{-2}	1.42×10^{-2}
10	1	4.09×10^2	3.05×10^2	119	69	2.01×10^{-1}	1.89×10^{-2}
11	23.7	1.03×10^4	3.25×10^2	8	32	1.60×10^{-1}	1.35×10^{-2}
12	282.1	2.23×10^5	5.92×10^2	25	58	2.02×10^{-1}	2.00×10^{-2}
13	107.7	6.35×10^4	4.54×10^2	17	92	2.07×10^{-1}	1.87×10^{-2}
Chelex 100							
1	1	6.09×10^1	4.41×10^1	15	40	8.67×10^{-2}	2.19×10^{-2}
2	51.3	6.58×10^3	9.28×10^1	42	83	1.87×10^{-1}	1.60×10^{-2}
3	1	9.77×10^1	7.08×10^1	35	24	1.30×10^{-1}	3.48×10^{-3}
4	1	2.49×10^2	1.80×10^2	63	62	1.46×10^{-1}	1.37×10^{-2}
Amberlite CG 50							
1	1.8	3.52×10^2	6.94×10^1	65	98	5.11×10^{-2}	
2	50.5	3.64×10^3	2.93×10^1	16	14	1.43×10^1	9.94×10^{-2}
3	563	9.16×10^5	3.62×10^2	453	325	3.25×10^2	4.50×10^{-2}

bt: Values obtained from the bt curve at $C/C_0 = 0.5$.

Comparing V_R of exp. IC Chelate, 1 and 9, with 6 and 11, which were carried out at similar conditions except a small temperature difference, but at different flow rate, it is seen that V_R is lower at higher elution rate, the difference being 31% and 52% in the two couples of experiments. The experiment at lower flow rate was always nearer to V_{Rcalc} than that at higher flow rate. This agrees with previous observations [8], but is not predicted by the simple model applied, based on the assumption that the concentration of free active groups is constant, being the sorbed metal ion at trace level. It is possible that the active groups at the surface of the particles are rapidly occupied by Cu(II), causing a local saturation of the active groups, which reduces λ', according to Eq. (13). The saturation of the active sites seems to take place earlier at lower pH when the deprotonated active groups in the resin are at very low concentration.

Another part of the bt profile related to the adsorption equilibrium is when the concentration in the outlet solution is equal to that of the inlet solution. This can be considered an equilibrium condition [7,8,32–34], since the concentration does not change in the two phases. Eq. (13) can be used to evaluate the free copper(II) concentration in the presence of total metal ion concentration C_0, from the concentration of copper(II) adsorbed on the resin. In Fig. 3 the free metal ion concentration evaluated by Eq. (13) is compared with $[Cu^{2+}]$ calculated from the side reaction coefficients reported in Table 2.

The comparison is:

$$\log[Cu^{2+}]_{calc} = -0.5(3) + 0.94(4)\ \log[Cu^{2+}]_{exp};$$

$$r^2 = 0.970 \quad (n = 18)$$

The fairly good agreement confirms that the proposed model for the sorption equilibria of copper(II) on the considered resins is useful even in relatively irreproducible columns as those of SPE procedures, making possible a fairly accurate prediction of D and V_R.

While the sorbing properties of a complexing resin can be well predicted by the proposed method, the prediction of V_R is possible only if the complexation state of the metal ion in solution is known too [30].

3.2. Adsorption kinetics in column

The kinetics of the sorption of copper(II) on complexing resin columns determines the parameter kC_0/Q (mL^{-1}) of Eq. (3), which represents the slope of the bt profile at the half exhaustion point [10]. When the bt curve is symmetrical with respect to V_R, as in the case of Amberlite CG 50, one kinetic parameter is obtained. In the case of the microporous iminodiacetic microporous resins the evaluation of the kinetic parameters was made separately for the two parts of the bt curve, as done for V_R, obtaining two different values of kC_0 (min^{-1}), as reported in Table 2.

Differently from the equilibrium parameters, the kinetic parameter depends on the temperature, according to the Arrhenius law:

$$\log kC_0 = -5.0(7) \times 10^3 \frac{1}{T} + 16(2); \quad r^2 = 0.81 \quad (n = 13) \qquad (15)$$

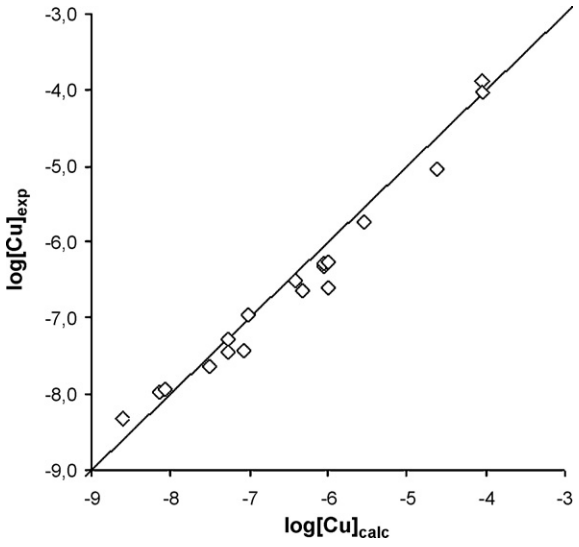

Fig. 3. Comparison of the free copper(II) concentration calculated from the known equilibria in solution and the free copper(II) concentration obtained by Eq. (13) from copper(II) concentration adsorbed on the resin at equilibrium conditions.

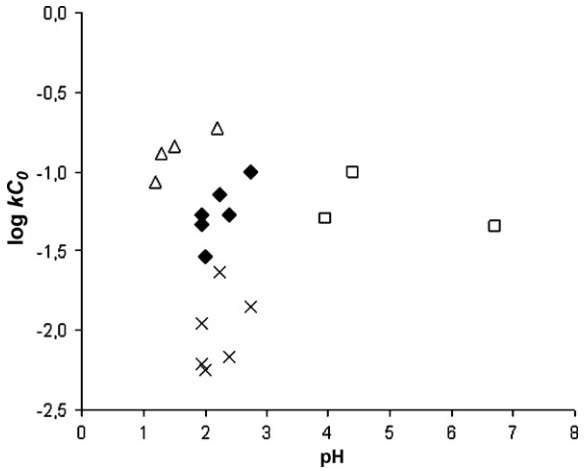

Fig. 4. Kinetic parameter kC_0 from breakthrough profiles of copper(II) at different pH, at $T = 293 \pm 2$ °K. △: Chelex 100, first part of the bt profile; ♦: IC Chelate, first part of the bt profile; ×: IC Chelate, second part of the bt profile; □: Amberlite CG 50, whole bt profile.

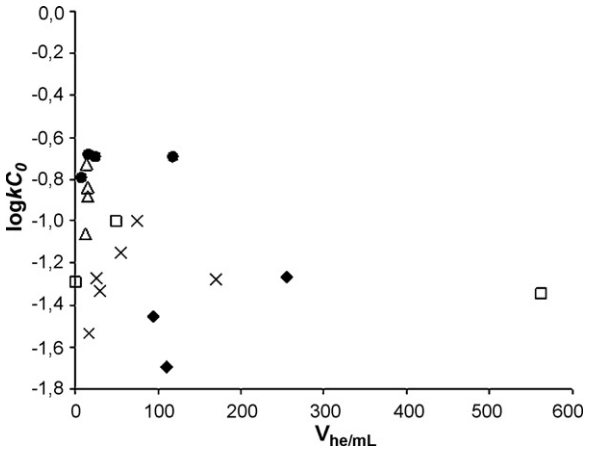

Fig. 5. Kinetic parameter kC_0 from breakthrough profiles of copper(II) at variuos half exhaustion volumes. △: Chelex 100, first part of the bt profile; ♦: IC Chelate, first part of the bt profile, $T = 290$ °K; ×: IC Chelate, first part of the bt profile, $T = 293$ °K; ●: IC Chelate, first part of the bt profile, $T = 303$ °K; □: Amberlite CG 50, whole bt profile, at rt.

The high irreproducibility is due to the different conditions at which the experiments were carried out, and probably also to the poor control of the temperature. In Fig. 4 some kinetic constants obtained at similar temperature (293 °K) are reported as function of the solution acidity.

The kinetic constants kC_0 of Amberlite CG 50 and of the first part of the bt curve of the iminodiacetic resins are very near, indicating that the rate limiting step in the first part of the bt curve is the same for the two resins, probably the ion exchange at the external particle surface. The kinetic constants in the second part of the elution profile for IC Chelate are reported in Fig. 4 too. They are lower than in the first part, suggesting that in the second part the rate limiting step is the diffusion in micropores, in which the diffusion coefficient is smaller than in the external diffusion layer.

The acidity and the ionic composition of the solution phase does not seem to significantly influence the kinetic parameters, while it highly affects the adsorption equilibria, since the adsorption is essentially an ion exchange. However it will be shown by batch procedure that the acidity has an influence on the kinetics too. Probably the experimental irreproducibility of SPE is too high to make those possible an accurate investigation of the effects of the solution composition.

The sorption kinetics from solutions at different concentrations of copper(II) was examined, sometimes in the presence of ligands. The kinetic parameter does not seem to be significantly affected, as seen for example comparing exp. IC Chelate 10, without ligands, with experiments 11, 12, 13, carried out in the presence of ligand, which significantly affects the concentration of the free metal ion, as seen from the side reaction coefficients reported in Table 2.

From the results in Table 2 and Fig. 4 it is seen that there is a high irreproducibility in the kinetic parameters. In Fig. 5 the kinetic parameters are reported as function of the experimental retention volume, which is related to the column efficiency by the well known relation

$$N = 16\left(V_R/W\right)^2$$

N is the number of theorical plates and W is the width of the chromatographic peak at the base. The irreproducibility is much higher at low V_R, lower than around 200 mL, corresponding to about 100 theoretical plates.

Considering the experiments in which V_R is higher than 100 mL, at around 20 °C, the average value of the kinetic constant is 0.051(5) min^{-1}. From this value it can be calculated by Eq. (3) that $V_R - V_b$ is about 40 mL at $Q = 1$ mL min^{-1}, considering as bt volume the eluted volume for which 10% of the total concentration emerges from the column. This value is higher than the retention volume in some of the experiments considered, particularly at low pH.

3.3. Batch sorption of copper(II) on complexing resins

Some examples of kinetic sorption curves of copper(II) on complexing resins obtained by batch procedure are shown in Fig. 6, where the metal fraction adsorbed is reported as function of time.

Several experiments at different conditions were carried out, as reported in Table 3. In all the experiments the amount of metal ion was largely below the total active groups in the considered resins. The fractions of copper(II) adsorbed at equilibrium (f_e) are reported in Table 4, together with those predicted from the partition coefficient λ' (f_{calc}) as previously described [22]:

$$f_{calc} = \frac{1}{1 + (\alpha_M V_{sol}/\lambda' w)} \quad (16)$$

V_{sol} is the volume of the solution phase and the other symbols have the same meaning as in the column experiments. The partition coefficient λ' was calculated from the internal complexation and protonation constants of the resin, as in the column experiments, as was the side reaction coefficient, α_M. Both λ' and α_M are reported in Table 4. The agreement between the fraction of adsorbed copper(II) calculated and that experimentally obtained is good. Most often the fraction of copper(II) adsorbed was near to 1 at the considered conditions, only in the case of Amberlite CG 50 fractions of adsorbed metal ion sometimes much lower than 1 were considered. It is seen that the fraction of adsorbed metal ion at equilibrium is predictable at different conditions on the basis of the Gibbs–Donnan model.

The consistency of the model can be checked by comparing the free copper(II) concentration evaluated by Eq. (13), from the concentration of copper(II) adsorbed in the resin, and that calculated from the complexation constants of Cu(II) with IDA in aqueous solution reported in the literature. These values are shown in Table 4. The comparison is:

$$[M]_{exp} = -0.8(9) + 0.8(2)[M]_{calc}; \quad r^2 = 0.701 \quad (n = 8)$$

As for the adsorption kinetics, it is seen in Fig. 6 that the kinetic behaviour of the two kinds of resin is quite different, as it was in the column experiments. With Amberlite CG 50 the equilibrium is reached after about 60 min in the pH range considered, while a much longer equilibration time is required for the microporous

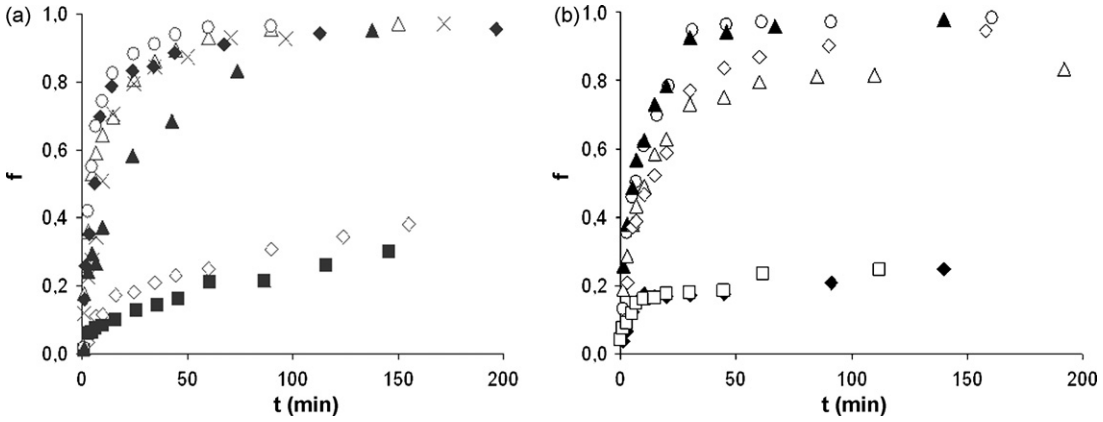

Fig. 6. Sorption curves of copper(II) on complexing resins by batch equilibration. The fraction of adsorbed metal ion is reported as function of time at different pH. (a) IC Chelate (0.500 g of dry resin); 0.1 M $NaNO_3$; $C_{Cu} = 2.1 \times 10^{-3}$ M: ♢: pH 1.96; ■: pH 2.16; △: pH 3.60, ♦: pH 3.90, $C_{IDA} = 5.0 \times 10^{-2}$ M; ○: pH 4.30; ▲: pH 4.80; ×: pH 6.05. (b) Amberlite CG 50 (0.300 g of dry resin); 0.1 M $NaNO_3$; $C_{Cu} = 5.1 \times 10^{-4}$ M: ♦: pH 3.24; △: pH 3.73, □: pH 4.52, $C_{IDA} = 6.7 \times 10^{-4}$ M; ○: pH 5.03; ▲: pH 5.45; ♢: pH 6.36.

iminodiacetic resins particularly at pH lower than 2.5. The kinetic constant k_k defined in Eq. (7), was obtained by Eq. (8). In the case of Amberlite CG 50 all the points lie on a single straight line passing through zero, while in the case of the iminodiacetic resins two distinct straight lines were obtained. The first one, at time periods shorter than 5 min, has slope similar to that of Amberlite CG 50, while the second one, at longer time, has a lower slope, indicating that a different diffusion, probably in the micropores, is rate limiting. The kinetic constants k_k obtained by Eq. (8) are reported in Table 4. In some of the experiments with Chelex 100 only the second straight line was detected, not passing through zero, because only long time periods have been considered. This behaviour is similar to that previously reported for the sorption of copper(II) and zinc(II) on Chelex 100 and IRC 748 [27].

In general the kinetic parameters k_k in Table 4 are similar to kC_0 determined by the column procedure at the same temperature. The

Table 3
Experimental conditions of adsorption of copper(II) on complexing resins by batch procedure, in $NaNO_3$ 0.10 M.

Experiment	T (°K)	Dry resin (g)	Stirring rate (rot min^{-1})	c_{Cu} (M)	c_{IDA} (M)	pH
IC Chelate						
1	291	0.4766	108	1.93×10^{-5}		2.05
2	290	0.4849	104	2.20×10^{-3}		2.58
3	290	0.4824	104	2.30×10^{-3}	5.11×10^{-2}	2.88
4	294	0.4836	104	2.08×10^{-3}		1.96
5	295	0.4553	104	2.24×10^{-3}	5.00×10^{-2}	2.16
6	295	0.4712	104	2.09×10^{-3}		3.60
7	295	0.4601	104	2.13×10^{-3}	5.10×10^{-2}	3.90
8	295	0.4742	104	2.09×10^{-3}		4.30
9	294	0.4750	104	2.21×10^{-5}		4.80
10	294	0.4720	104	2.19×10^{-5}		6.03
11	295	0.4483	172	2.24×10^{-3}		2.00
12	298	0.4480	76	2.23×10^{-3}		1.94
13	298	0.4971	104	2.16×10^{-4}		2.27
Chelex 100						
1	291	0.4877	104	1.97×10^{-3}	4.98×10^{-2}	2.03
2	291	0.4409	104	1.92×10^{-3}		2.06
3	291	0.4617	104	2.19×10^{-3}	5.00×10^{-2}	2.51
4	291	0.4294	104	2.06×10^{-3}	5.00×10^{-2}	2.54
5	291	0.4779	104	2.11×10^{-3}	5.00×10^{-2}	2.55
6	291	0.4237	104	2.20×10^{-3}		2.83
7[a]	298	0.5224	104	4.85×10^{-4}		2.00
Amberlite CG 50						
1	295	0.3106	104	4.96×10^{-4}		3.24
2	295	0.3103	104	5.19×10^{-4}		3.73
3	295	0.2986	104	4.97×10^{-4}	6.76×10^{-4}	4.52
4	295	0.3109	104	5.08×10^{-4}		5.03
5	295	0.2967	104	5.08×10^{-4}		5.45
6	295	0.3017	104	5.13×10^{-4}		6.35
7	295	0.2951	288	5.09×10^{-4}		4.75
8	295	0.1066	288	5.06×10^{-4}		5.23
9[a]	298	0.3107	104	4.87×10^{-4}		3.80
10	298	0.1089	104	5.22×10^{-4}		3.92
11	298	0.2835	104	1.61×10^{-3}		4.63
12	298	0.1066	104	5.25×10^{-4}		5.72
13	298	0.2841	68	5.16×10^{-4}		4.50
14	298	0.2860	76	5.23×10^{-4}		4.50
15	298	0.2821	184	5.23×10^{-4}		4.52

[a] 1.00 M $NaNO_3$.

Table 4
Equilibria and kinetics of adsorption of copper(II) on complexing resins determined from the adsorption curves of copper(II) on complexing resins by batch procedure. The experimental conditions are reported in Table 3.

Experiment	α_M	f_{calc}	f_{exp}	k_k (I)	k_k (II)	$\log[M]_{exp}$	$\log[M]_{calc}$
IC Chelate							
1	1	1.00	0.98		3.8×10^{-3}		
2	1	1.00	0.98	3.8×10^{-2}	8.5×10^{-3}		
3	861	0.94	0.86	2.4×10^{-2}	2.3×10^{-3}		
4	1	0.99	0.89	1.2×10^{-2}	1.8×10^{-3}		
5	24	0.87	0.66	1.5×10^{-2}	1.8×10^{-3}	5.0	−4.5
6	1	1.00	0.99	1.4×10^{-1}	2.4×10^{-2}		
7	1210	0.99	0.98	1.3×10^{-1}	1.9×10^{-2}		
8	1	1.00	0.99	1.8×10^{-1}	3.8×10^{-2}		
9	1	1.00	0.97	8.7×10^{-2}	2.4×10^{-2}		
10	1	1.00	0.97	8.3×10^{-2}	2.3×10^{-2}		
11	1	0.99	0.87	3.1×10^{-2}	4.0×10^{-3}		
12	1	0.99	0.93	1.8×10^{-2}	3.0×10^{-3}		
13	1	1.00	0.93	6.8×10^{-2}	9.6×10^{-3}		
Chelex 100							
1	24	0.64	0.83		5.6×10^{-3}	−4.4	−4.8
2	1	0.97	0.95		5.4×10^{-2}		
3	154	0.74	1.00		9.3×10^{-3}		
4	154	0.72	0.85		7.7×10^{-3}	−5.3	−5.7
5	154	0.74	0.91		8.9×10^{-3}		
6	1	0.99	0.99		1.6×10^{-2}		
7	1	0.97	0.95	3.4×10^{-1}	1.7×10^{-2}		
Amberlite CG 50							
1	1	0.32	0.22	1.5×10^{-1}		−3.6	−3.4
2	1	0.74	0.86	5.6×10^{-2}		−3.8	−4.1
3	1	0.32	0.26	7.2×10^{-2}		−3.5	−3.4
4	1	1.00	0.98	6.7×10^{-2}			
5	1	1.00	0.99	7.3×10^{-2}			
6	1	1.00	1.00	5.9×10^{-2}			
7	1	0.99	1.00	6.2×10^{-1}			
8	1	1.00	1.00	5.4×10^{-1}			
9	1	0.59	0.89	2.1×10^{-1}		3.5	4.3
10	1	0.67	0.60	9.2×10^{-2}		3.8	3.7
11	1	0.99	0.99	1.4×10^{-1}			
12	1	1.00	1.00	1.2×10^{-1}			
13	1	0.98	0.97	3.6×10^{-2}			
14	1	0.98	1.00	4.3×10^{-2}			
15	1	0.98	0.98	7.1×10^{-1}			

Arrhenius law for experiments at similar conditions, i.e. at a stirring rate of 104 rot min^{-1}, in 0.1 M $NaNO_3$, and pH higher than 3 is:

$\log k_k = -6(2)\times10^3\left(\frac{1}{T}\right) + 20(6)$; $r^2 = 0.51$ (n = 14, grouped in three temperature clusters) .

The parameters of the above relationship are similar to those obtained by column procedure (see Eq. (15)), where the dependence of the kinetic parameter kC_0 from temperature was considered.

Several different conditions were tested, obtaining largely different kinetic parameters. They should vary according to Eq. (7). The effect of the counter ion concentration on the kinetic constant can be observed by comparing the experiments in 1 M $NaNO_3$ with similar experiments in 0.1 M $NaNO_3$, reported in Table 4, for example exp Chelex 100 7, and IC Chelate 13, at pH ∼ 2.2 and t = 25 °C, and Amberlite CG 50 9 and 11, at pH ∼ 4 and t = 25 °C. The kinetic parameters are higher in 1 M than in 0.1 M for both the resins, the differences being respectively 0.27 and 0.077 min^{-1}.

The concentration of monovalent counter ion in the resin phase ($[\bar{B}]$) can be evaluated by the Gibbs–Donnan model, since the intrinsic protonation constants are known: 0.18 mmol g^{-1} in $NaNO_3$ 0.1 M and 1.10 mmol g^{-1} in 1 M $NaNO_3$ for Chelex 100 (at pH 2.2), and 0.405 mmol g^{-1} in 0.1 M $NaNO_3$ and 2.02 mmol g^{-1} in 1 M $NaNO_3$ for Amberlite CG 50 (at pH 4) [29]. The values of the forward kinetic constants were determined by solving the two equation systems. The results are: for iminodiacetic resins, k_f = 191 and for Amberlite CG 50, k_f = 112. They confirm that the same step is rate limiting for the adsorption of copper(II) on the two resins. Negative values were obtained for the backward constants, probably because they are too low to be correctly evaluated from only two data points, subjected to a considerable irreproducibility.

The knowledge of the forward constant makes possible to evaluate the kinetic constant k_k at different ionic compositions and acidity levels of the external solution.

According to Eq. (7), the solution acidity should affect the kinetic constant, since the concentration of free counter ions in the resin phase ($[\bar{B}]$) depends on the acidity and the ionic composition of the solution, as extensively described for the two kinds of resins here examined [22,29]. The effect of the acidity of the solution phase on the adsorption kinetics is shown in Fig. 7, in which the results of some experiments carried out at 104 rot min^{-1}, T = 291 °K and 295 °K, in $NaNO_3$ 0.1 M, are reported. At pH higher than 3.5, the kinetic parameter is independent of the solution acidity, while at lower pH it decreases with increasing acidity. Actually, if the active groups in the resins are monoprotonated, and if $\overline{K_{a1}}[H]$ is much higher than 1, the following relationship is obtained by substituting the concentration of counter ion in the resin in Eq. (7):

$$k_k = k_f \frac{w}{V}\frac{\overline{C_{tot}}}{K_a[H]} + k_b C_B^2 \frac{w}{V_s} \quad (17)$$

When the first term to the right in Eq. (17) is much higher than the second one, $\log k_k$ vs pH is a straight line with slope 1, while it is a line parallel to the abscissa at higher pH when the first term is negligible. The pH effect is clearly seen in batch experiments, while it could not be detected in the case of the column experiments (Fig. 5), probably due to the high irreproducibility of those experiments at low pH, and low V_R It is interesting that some aspects of

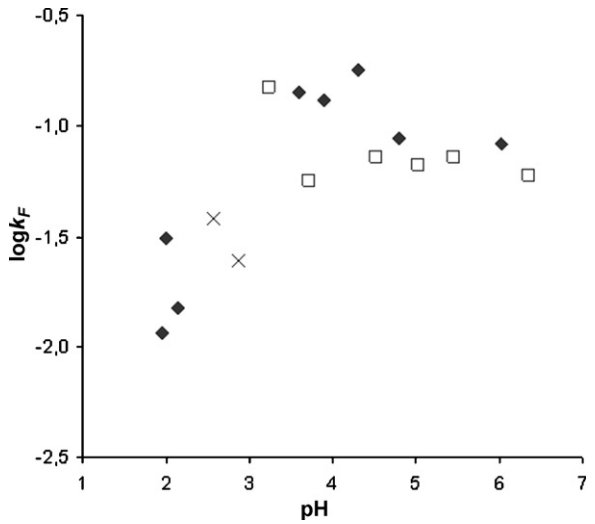

Fig. 7. Effect of the solution acidity on the kinetic constants of the sorption of copper(II) on complexing resins by batch equilibration, at 104 rot min^{-1}, 0.1 $NaNO_3$; ♦: IC Chelate, T = 295 °K; ×: IC Chelate, T = 290 °K; □: Amberlite CG 50, T = 295 °K. For IC Chelate, log k_k is that obtained in the first 5 min.

the adsorption kinetics can be well justified on the basis of equilibrium concepts, as for example the protonation of the weak acid groups in the resins phase.

Another variable that could have an influence on the kinetic parameter is the amount of resin per unit volume of solution (w/V in g_s mL^{-1}). This can be appreciated in the case of Amberlite CG 50 by comparing Exp. (8) and 9 (w/V = 0.0036) with Exp. (7) (w/V = 0.0094), at 104 rot min^{-1}, T = 298 °K, or Exp. (14) with Exp. (13) at 288 rot min^{-1}, T = 295 °K. The kinetic constant is slightly higher when the resin concentration is higher, particularly at lower rotation rate, but not as much as expected from Exp. (17). More investigation must be done to elucidate this point.

Several copper(II) concentrations were considered, from 2×10^{-5} M to 5×10^{-3} M, in the presence and in the absence of the ligand IDA. The total or free copper(II) concentration does not appear to affect the kinetic constant, neither does the presence of the ligand IDA, as seen by comparing, exp. IC Chelate 4 and 5 (at t = 22 °C, pH ∼ 2) with 7 and 6 (at t = 22 °C, pH ∼ 3.6), and exp. Amberlite CG 50 2 with 3. The differences are within the experimental uncertainty. The same was found in the dynamic adsorptions in column. It was previously documented for Chelex 100 and other metal collectors [39,40] that the exchange of complexed metal ions is slower than that of aquo-ions. However in the cases here examined the rate determining step is evidently not the dissociation of the copper(II) complexes, but the adsorption on the resin by ion exchange. Further investigation with different ligands must be carried out to clarify this point, which is important to transfer the concepts here described to unknown samples, as for example environmental waters. Besides the variables described above, the effect of which can be predicted by Eq. (7), the stirring rate too influences the kinetics, particularly in the case of Amberlite CG 50. This confirms that the ion exchange takes place at the external particle/solution interface, in the film at the particle surface. The proposed model is not able to predict this effect, however it has been found that at 104 rot min^{-1} kinetic parameters similar to those in column at elution rate around 1 mL min^{-1} are obtained. In a previous investigation on the batch adsorption of copper(II) on Chelex 100 [7], at 25 °C and not defined counter ion concentration in solution, the first order kinetic constant was found to be around 0.8 min^{-1}, not so different for the results of the experiment here carried out at the same temperature, and in 1 M $NaNO_3$, 0.3 min^{-1}.

The kinetic parameters evaluated at time periods longer than about 5 min are similar to the corresponding parameters obtained by column procedure, and so can be used for the prediction of the attainment of equilibrium conditions in column. These kinetic constants are less affected by the counter ion concentration than those in the first part of the adsorption curve, indicating that the rate determining step is different, possibly the diffusion in the pores. A complete investigation of the variables relevant for these constants was not here carried out.

4. Conclusions

Only seldom a comparison of the equilibrium and kinetic parameters of a sorption process from fixed bed and batch experiments has been carried out. For example in a recent paper [12] the two approaches were used, but the batch results were considered only for equilibrium characterization, and the column results only for kinetics. In the present investigation it has been demonstrated that both the equilibrium and the kinetic parameters characterizing the bt profile of copper(II) on complexing resin columns can be predicted at different conditions, such as ionic composition and acidity. It has been demonstrated that this was possible also in the case of small columns of complexing resins, similar to the cartridges used for solid phase extraction, with a relatively low number of theoretical plates. The retention volume V_R, which depends on adsorption equilibria, can be predicted in a wide range of conditions, by applying the Gibbs–Donnan model. The agreement between the experimental and calculated V_R is fairly good, considering the uncertainty in the evaluation of the exchange coefficients. The knowledge of a kinetic parameter is required for the evaluation of V_b. In the present investigation it has been found to be very similar for the three considered resins, due to the fact that the ion exchange in the external film is the rate limiting step, at least under the conditions here considered. The morphology of the resin, and in particular the presence of micropores, seems to influence mainly the second part of the elution profile, so it is not important for prediction of V_b. The effect of ionic strength and acidity of the solution on the kinetic constant has been investigated, and found to be in agreement with the hypothesis that the rate determining step for the adsorption of copper(II) is the ion exchange reaction, at least in the first part of the bt profile. A large irreproducibility is inherent to the SPE methods. Despite this, the feasibility of the prediction on the basis of completely independent determinations was here demonstrated for two different kinds of resins, the iminodiacetic and the carboxylic resin, both of which are widely used for SPE of metal ions.

Nomenclature

$[\bar{B}]$	concentration of the counter ion not linked to the active groups in the resin phase
C	outlet concentration of total metal ion
C_0	inlet concentration of total metal ion
C_B	concentration of a monovalent counter ion in the solution phase
$\overline{c_L}$	total concentration of free complexing groups in the resin
D	distribution coefficient, i.e. ratio of the total concentration of the metal ion in mobile and solution phase
k_k	kinetic constant of the ion exchange reaction in batch
kC_0	first order rate constant of the sorption reaction in column
k_f, k_b	forward and reverse rate constants
$\overline{K_{ay}}$	apparent protonation constants of the complexing groups in the resin
K_i	complexation constant in the resin phase

q_e concentration of the metal ion in the resin phase at equilibrium with C_0
q_t concentration of metal ion in the resin phase at time t
Q volumetric flow rate
V_b breakthrough volume, i.e. eluted volume for which a low concentration of metal ion (for example 1–10% of the original concentration) emerges from the column
V_m volume of the mobile phase in column
V_R retention volume, i.e. eluted volume corresponding to the inflection point of the bt curve
V_s volume of the stationary phase in column
w mass of resin in column and batch experiments
$X = q_t/q_e$ the fractional approach to equilibrium

Greek symbols
$\overline{\alpha_{H_xL}}$ side reaction coefficient of the x-protonated groups H_xL in the resin phase
α_M side reaction coefficient of the metal ion in solution, i.e. ratio of total to free metal ion in solution
β deprotonation degree of the active groups in the resin
λ' ratio of the concentration of all the metal species in the resin phase to the free metal ion in solution, at equilibrium

Acknowledgement

This work was financially supported in part by PNRA (Programma Nazionale di Ricerche in Antartide)-PEA2006 (Italy).

References

[1] J.P. Riley, D. Taylor, Anal. Chim. Acta 40 (1968) 479.
[2] R. Biesuz, G. Alberti, G. D'Agostino, E. Magi, M. Pesavento, Mar. Chem. 101 (2006) 180.
[3] F. Baffi, A.M. Cardinale, R. Bruzzone, Anal. Chim. Acta 270 (1992) 79.
[4] Y. Sohrin, S. Urushihara, S. Nakatsuka, T. Kono, E. Higo, T. Minami, K. Norisuye, S. Umetani, Anal. Chem. 80 (2008) 6267.
[5] S. Motellier, H. Pitsch, J. Chromatogr. A 739 (1996) 119.
[6] P.R. Haddad, P. Doble, M. Macka, J. Chromatogr. A 856 (1999) 145.
[7] P. Sajonz, G. Zhong, G. Guiochon, J. Chromatogr. A 728 (1996) 15.
[8] P. Sajonz, M. Kele, G. Zhong, B. Sellergren, G. Guiochon, J. Chromatogr. A 810 (1998) 1.
[9] A. Andrzejewska, K. Kaczmarski, G. Guiochon, J. Chromatogr. A 1216 (2009) 1067.
[10] M. Ruiz, A.M. Sastre, M.C. Zikan, E. Guibal, J. Appl. Polym. Sci. 81 (2001) 153.
[11] R.S Juang, H.C. Kao, W. Chen, Sep. Purif. Technol. 49 (2006) 36.
[12] L.C. Lin, J.K. Li, R.S. Juang, Desalination 225 (2008) 249.
[13] F. Helfferich, Ion Exchange, McGraw-Hill, New York, 1962 (Chapter 5, p. 140).
[14] M. Pesavento, R. Biesuz, G. Alberti, M. Sturini, J. Sep. Sci. 26 (2003) 381.
[15] M. Pesavento, A. Profumo, A. Sastre, Talanta 41 (1994) 1689.
[16] F. Helfferich, Ion Exchange, McGraw-Hill, New York, 1962 (Chapter 9, p. 466).
[17] M.C. Hennion, C. Cau-Dit-Coumes, V. Pichon, J. Chromatogr. A 823 (1998) 147.
[18] M. Pesavento, R. Biesuz, A. Alberti, Dalla Riva, React. Funct. Polym. 46 (2001) 233.
[19] Y. Merle, J. Marinsky, Talanta 31 (1984) 199.
[20] J.A. Marinksy, T. Miyajima, E. Högfeldt, M. Muhammed, React. Polym. 11 (1989) 279.
[21] L.-C. Lin, R.-S. Juang, Chem. Eng. J. 112 (2005) 211.
[22] M. Pesavento, R. Biesuz, M. Gallorini, A. Profumo, Anal. Chem. 65 (1993) 2522.
[23] M. Pesavento, R. Biesuz, J.L. Cortina, Anal. Chim. Acta 298 (1994) 225.
[24] S.H. Lin, C.D. Kiang, Chem. Eng. J. 92 (2003) 193.
[25] Z. Aksu, F. Gönen, Process Biochem. 39 (2004) 599.
[26] M.A. Fernandez, W.S. Laughinghouse, G. Carta, J. Chromatogr. A 746 (1996) 185.
[27] L.C. Lin, R.S. Juang, Chem. Eng. J. 132 (2007) 205.
[28] J.L. Cortina, A. Warshawsky, N. Kahana, V. Kampel, C.H. Sampaio, R.M. Kautzmann, React. Funct. Polym. 54 (2003) 23.
[29] R. Biesuz, M. Pesavento, G. Alberti, F. Dalla Riva, Talanta 55 (2001) 541.
[30] M. Pesavento, E. Baldini, Anal. Chim. Acta 389 (1999) 59.
[31] M. Pesavento, A. Profumo, R. Biesuz, G. Alberti, Solvent Extract. Ion Exchange 26 (2008) 301.
[32] F.F. Cantwell, J.S. Nielsen, S.E. Hrudey, Anal. Chem. 54 (1982) 1498.
[33] K.C. Bowles, S.C. Apte, G.E. Batley, L.T. Hales, N.J. Rogers, Anal. Chim. Acta 558 (2006) 237.
[34] I.A.M. Worms, K.J. Wilkinson, Anal. Chim. Acta 16 (2008) 95.
[35] M.L. Brusseau, R.E. Jessup, P.S.C. Rao, Environ. Sci. Technol. 25 (1991) 134.
[36] M.L. Brusseau, Q. Hu, R. Srivastava, J. Contam. Hydrol. 24 (1997) 205.
[37] J. Puigdomenec, MEDUSA: Make Equilibrium Diagram Using Sophisticated Algorithm. Windows Program, Stockholm vers 21, 2001.
[38] R. Biesuz, M. Pesavento, A. Gonzalo, M. Valiente, Talanta 47 (1998) 127.
[39] P. Burba, P.G. Willmer, Fresenius, J. Anal. Chem. 342 (1992) 167.
[40] P. Burba, J. Rocha, D. Klockow, Fresenius, J. Anal. Chem. 349 (1994) 800.